IEICE TRANS. FUNDAMENTALS, VOL.E91–A, NO.8 AUGUST 2008

PAPER Special Section on Signal Processing

Throughput Improvement with Discrete Pilot Signal Assignment and Iterative Channel Identification for MQRD-PCM/OFDM

Chang-Jun AHN[†a)], ***Member***

SUMMARY In MIMO systems, the channel identification is important to distinguish transmitted signals from multiple transmit antennas. One of the most typical channel identification schemes is to employ a code division multiplexing (CDM) based scheme in which a unique spreading code is assigned to distinguish both BS and MS antenna elements. However, by increasing the number of base stations and transmit antenna elements, large spreading codes and pilot symbols are required to distinguish the received power from all the connectable BS, as well as to identify all the CSI for the combination of transmitter and receiver antenna elements. Furthermore, the complexity of maximum likelihood detection (MLD) for implementation of MIMO is a considerable work. To reduce these problems, in this paper, we propose the parallel detection algorithm using multiple QR decompositions with permuted channel matrix (MQRD-PCM) with discrete pilot signal assignment and iterative channel identification for MIMO/OFDM.

key words: *MIMO, OFDM, QR decomposition, MQRD-PCM*

1. Introduction

For wireless communications with a limited amount of bandwidth, more spectrum efficient techniques are required. Multiple-input multiple-output (MIMO) is one of the most promising techniques for achieving more efficient bandwidth utilization, since it enable the transmission rate over MIMO channels to be increased by using multiple antennas on both the transmitter and receiver sides [1], [2]. Maximum likelihood detection (MLD), which is the best performing scheme, generates replicas of the received signals from candidates of the desired and co-channel interference(CCI) signals [3]–[6]. However, the complexity of MLD exponentially increases with the constellation size and the number of transmitter antenna branches. Accordingly, it is impractical to use a full MLD without reducing its computational complexity, because it would be prohibitively large for implementation. Regarding the problem of implementation, a promising approach that applies QR decomposition in association with an M-algorithm to MLD has been proposed as QRD-M [7]–[10].

The QRD-M scheme produces approximately the same BER as a full MLD using soft-decision decoding. QRD-M decomposes the channel response matrix H into a unitary matrix Q and an upper triangular matrix R. Since Q is unitary, multiplication of Q^H and the received signal vector has no noise enhancement, and the noise vector will still be white after unitary transformation. Therefore, QRD-M achieves a superior system performance using soft-decision decoding [11]. However, the performance of QRD-M depends on the number of surviving symbol replica candidates. When QRD-M uses a small number of candidates, the performance is degraded. On the other hand, when there is a large number of surviving symbol replica candidates and the transmitter antenna branches, QRD-M requires a large memory to maintain the branch metrics for the surviving symbol replicas. Moreover, in the QRD-M algorithm, tentative decisions on the symbols are made serially, but the final decision is jointly made. Thus, instead of searching for all combinations, the search is limited by pruning the search tree in a breadth-first manner. In this case, the QRD-M is similar to serial detection methods. Thus, long latency time is also required. Recently, the parallel detection algorithm using multiple QR decompositions with permuted channel matrix for MIMO/OFDM (MQRD-PCM/MIMO-OFDM) has been proposed [12].

Moreover, in MIMO systems, the channel identification is important to distinguish transmitted signals from multiple transmit antennas. Several algorithms are proposed to distinguish transmitted signals [13], [14]. One of the most typical channel estimation schemes is to employ a code division multiplexing (CDM) based scheme in which a unique spreading code is assigned to distinguish both BS and MS antenna elements [15], [16]. However, by increasing the number of base stations and transmit antenna elements, large spreading codes and pilot symbols are required to distinguish the received power from all the connectable BS, as well as to identify all the CSI for the combination of transmitter and receiver antenna elements. In this case, the throughput performance is also degraded since the pilot symbol does not carry any information. In fact, the channel response at a particular subcarrier frequency is not supposed to be totally different from its neighboring frequencies, and hence, they must have correlation which depends on the coherence bandwidth of the channel B_c [17]. If we consider the discrete pilot signal assignment for identifying all the CSI for the combination of transmitter and receiver antenna elements with reduced pilot symbols, the throughput performance is not degraded. To reduce the above-mentioned problems, in this paper, we consider the discrete pilot signal assignment and an iterative channel identification for MQRD-PCM/MIMO-OFDM to improve the total throughput. This paper is organized as follows. The configuration of the proposed MIMO/OFDM system is described in Sect. 2. In Sect. 3, we show the computer simulation results. Finally,

Manuscript received November 30, 2007.
Manuscript revised March 5, 2008.

[†]The author is with the Faculty of Information Sciences, Hiroshima City University, Hiroshima-shi, 731-3194 Japan.
a) E-mail: junny@m.ieice.org

DOI: 10.1093/ietfec/e91–a.8.2000

the conclusion is given in Sect. 4.

2. Proposed MIMO/OFDM System

This section describes the proposed MIMO/OFDM system, which employs time division multiplexing (TDM) transmission for multiple users. The proposed MIMO/OFDM system is illustrated in Fig. 1.

2.1 Channel Model

We assume that the propagation channel consists of L discrete paths with different time delays. The impulse response between the mth transmitter and the nth receiver antenna $\hbar_{m,n}(\tau, t)$ is represented as

$$\hbar_{m,n}(\tau, t) = \sum_{l=0}^{L-1} \hbar_{m,n,l}(t)\delta(\tau - \tau_{m,n,l}), \tag{1}$$

where $\hbar_{m,n,l}$, $\tau_{m,n,l}$ are the complex channel gain and the time delay of the lth propagation path, respectively. The channel transfer function $h_{m,n}(f, t)$ is the Fourier transform of $\hbar_{m,n}(\tau, t)$ and is given by

$$\begin{aligned} h_{m,n}(f, t) &= \int_0^{\infty} \hbar_{m,n}(\tau, t) \exp(-j2\pi f\tau) d\tau \\ &= \sum_{l=0}^{L-1} \hbar_{m,n,l}(t) \exp(-j2\pi f\tau_{m,n,l}). \end{aligned} \tag{2}$$

2.2 Proposed MIMO/OFDM Transmitter

The transmitter block diagram of the proposed MIMO/OFDM system is shown in Fig. 1(a). Firstly, the coded binary information data sequence is modulated, and N_p pilot symbols are appended at the beginning of the sequence. The proposed MIMO/OFDM transmit signal for the mth transmit antenna can be expressed in its equivalent baseband representation as

$$\begin{aligned} s_m(t) = &\sum_{i=0}^{N_p+N_d-1} g(t - iT) \cdot \sqrt{\frac{2S}{N_c}} \sum_{k=0}^{N_c-1} x_m(k, i) \\ &\cdot \exp\left[j2\pi(t - iT)k/T_s\right], \end{aligned} \tag{3}$$

where N_d and N_p are the number of data and pilot symbols, N_c is the number of carriers, T_s is the FFT time length, S is the average transmitting power, T is the OFDM symbol length, respectively. The frequency separation between adjacent orthogonal subcarriers is $1/T_s$ and can be expressed, by using the kth subcarrier of the ith modulated symbol $x_m(k, i)$ with $|x_m(k, i)| = 1$ for $N_p \le i \le N_p + N_d - 1$. The guard interval T_g is inserted in order to eliminate the intersymbol interference (ISI) due to the multipath fading, and hence, we have

$$T = T_s + T_g. \tag{4}$$

In Eq. (3), $g(t)$ is the transmission pulse given by

$$g(t) = \begin{cases} 1 & \text{for } -T_g \le t \le T_s \\ 0 & \text{otherwise.} \end{cases} \tag{5}$$

For $N_p = 2$ and $M = 4$ where M is the number of transmit antenna elements, the transmitted pilot signal of the kth subcarrier of the mth transmit antenna element is given by

$$d_m(k, i) = \begin{cases} \Phi_1(i) & \text{for } \lceil \frac{m-1}{N_p} \rceil = 0 \mid \mathrm{mod}(k, N_p) = 0 \\ \Phi_2(i) & \text{for } \lceil \frac{m-1}{N_p} \rceil = 1 \mid \mathrm{mod}(k, N_p) = 1 \\ \Phi_0(i) & \text{otherwise,} \end{cases} \tag{6}$$

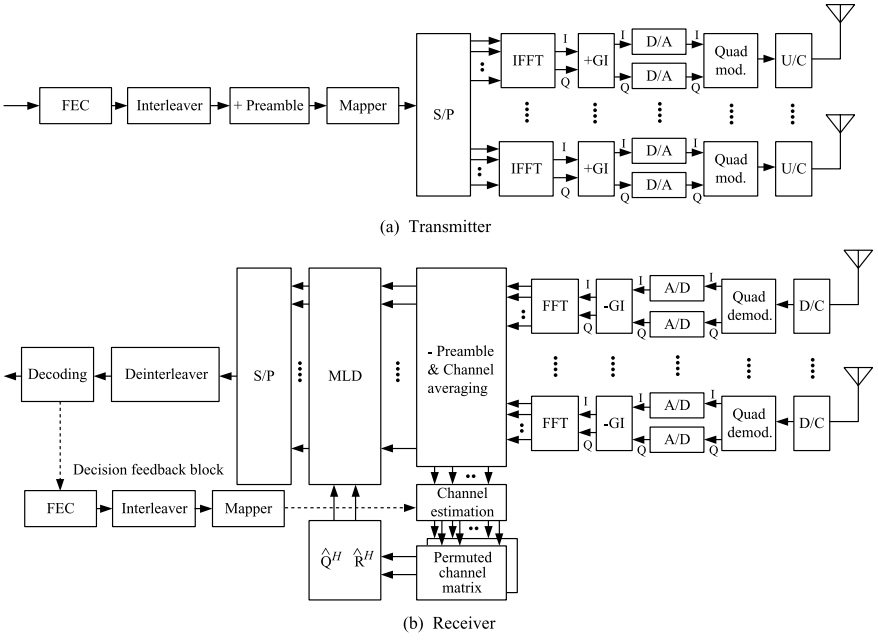

Fig. 1 Proposed MIMO/OFDM system.

where Φ is the orthogonal spreading code as $\Phi_1 = (1,1)$, $\Phi_2 = (1,-1)$, $\Phi_0 = (0,0)$, "mod" means the modulus, $\lceil x \rceil$ denotes the smallest integer more than or equal to x, and | denotes the logical operator "AND," respectively. For simplicity, in this paper, we consider 4×4 MIMO system. The transmitted pilot signal of the kth subcarrier of the mth transmit antenna element is given in Fig. 2.

2.3 Receiver Structure

The receiver structure is illustrated in Fig. 1(b). By applying the FFT operation, the received signal $y(t)$ is resolved into N_c subcarriers. The received signal for the nth received antenna $y_n(t)$ in the equivalent baseband representation can be expressed as

$$y_n(t) = \sum_{m=0}^{M-1} \int_{-\infty}^{\infty} \hbar_{m,n}(\tau, t) s_m(t-\tau) d\tau + \nu_n(t), \tag{7}$$

where $\nu_n(t)$ is additive white Gaussian noise (AWGN) with a single sided power spectral density of N_0 for the nth received antenna. The kth subcarrier $y_n(k,i)$ is given by

$$\begin{aligned} y_n(k,i) &= \frac{1}{T_s} \int_{iT}^{iT+T_s} y_n(t) \\ &\quad \cdot \exp\left[-j2\pi(t-iT)k/T_s\right] dt \\ &= \sqrt{\frac{2S}{N_c}} \sum_{m=0}^{M-1} \sum_{e=0}^{N_c-1} x_m(e,i) \\ &\quad \frac{1}{T_s} \int_0^{T_s} \exp[j2\pi(e-k)t/T_s] \\ &\quad \cdot \left\{ \int_{-\infty}^{\infty} \hbar_{m,n}(\tau, t+iT) g(t-\tau) \right. \\ &\quad \left. \cdot \exp(-2\pi e\tau/T_s) d\tau \right\} dt + \nu_n(k,i), \end{aligned} \tag{8}$$

where $\nu_n(k,i)$ is AWGN noise with zero-mean and a variance of $2N_0/T_s$. Assuming that the maximum $\tau_{m,n,l}$ is shorter than the guard interval T_g, the integral with respect to τ becomes, from Eq. (5),

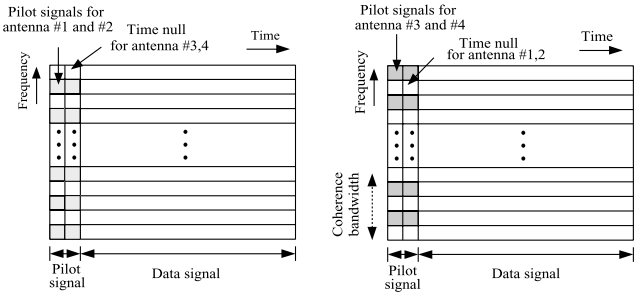

(a) Pilot signal assignment for transmitting data from antenna # 1,2

(b) Pilot signal assignment for transmitting data from antenna # 3,4

Fig. 2 Pilot signal assignment.

$$\begin{aligned} &\int_{-\infty}^{\infty} \hbar_{m,n}(\tau, t+iT) g(t-\tau) \exp(-j2\pi e\tau/T_s) d\tau \\ &= \int_0^{T_s} \hbar_{m,n}(\tau, t+iT) \exp(-j2\pi e\tau/T_s) d\tau \\ &= h_{m,n}(e, t+iT). \end{aligned} \tag{9}$$

Assuming that $h_{m,n}(t)$ remains almost constant over the symbol length T, we have

$$h_{m,n}(k, t+iT) \approx h_{m,n}(k, iT), \quad \text{for } 0 \le t \le T. \tag{10}$$

As a result, Eq. (8) can be rewritten as

$$\begin{aligned} y_n(k,i) &\approx \frac{1}{T_s} \sqrt{\frac{2S}{N_c}} \sum_{m=0}^{M-1} \sum_{e=0}^{N_c-1} x_m(e,i) \\ &\quad \int_0^{T_s} \exp[j2\pi(e-k)t/T_s] \\ &\quad \cdot \left\{ \int_{-\infty}^{\infty} \hbar_{m,n}(\tau, t+iT) g(t-\tau) \right. \\ &\quad \left. \cdot \exp(-2\pi e\tau/T_s) d\tau \right\} dt + \nu_n(k,i) \\ &= \sqrt{\frac{2S}{N_c}} \sum_{m=0}^{M-1} h_{m,n}(k, iT) x_m(k,i) \\ &\quad + \nu_n(k,i). \end{aligned} \tag{11}$$

The estimated channel impulse response of kth subcarrier between the mth transmitter and the nth receiver $h_{m,n}(k)$ is calculated by interpolation of the discretely assigned pilot signals as

$$h_{m,n}(k) = \begin{cases} \frac{1}{N_p} \sum_{i=0}^{N_p-1} y_n(k,i) \otimes \Phi_1(i) \\ \quad \text{for } \lceil \frac{m-1}{N_p} \rceil = 0 \mid \mathrm{mod}(k, N_p) = 0 \\ \frac{1}{N_p} \sum_{i=0}^{N_p-1} y_n(k,i) \otimes \Phi_2(i) \\ \quad \text{for } \lceil \frac{m-1}{N_p} \rceil = 1 \mid \mathrm{mod}(k, N_p) = 1 \\ \frac{h_{m,n}(k-1) + h_{m,n}(k+1)}{2} \\ \quad \text{for } \lceil \frac{m-1}{N_p} \rceil = 0 \mid \mathrm{mod}(k, N_p)_{k \ne N_c - 1} = 1 \\ \quad \text{or} \\ \quad \text{for } \lceil \frac{m-1}{N_p} \rceil = 1 \mid \mathrm{mod}(k, N_p)_{k \ne 0} = 0 \\ h_{m,n}(k-1) \quad \text{for } \lceil \frac{m-1}{N_p} \rceil = 0 \mid k = N_c - 1 \\ h_{m,n}(k+1) \quad \text{for } \lceil \frac{m-1}{N_p} \rceil = 1 \mid k = 0 \end{cases} \tag{12}$$

where $\otimes$ denotes convolution.

2.4 MQRD-PCM

Alternately, (11) can be written in matrix form as

$$Y(k) = H(k)X(k) + \nu(k) \quad k = 0, \cdots, N_c - 1 \tag{13}$$

where $Y(k)$ is the $N \times 1$ received signal matrix, $X(k)$ is the $M \times 1$ transmitted signal matrix, $H(k)$ is the $N \times M$ channel matrix where N is the number of received antennas, and $\nu(k)$ is the $N \times 1$ noise matrix. From Eq. (13), we can denote the signal model as

$$\begin{bmatrix} y_1(k) \\ y_2(k) \\ \vdots \\ y_N(k) \end{bmatrix} = \begin{bmatrix} h_{1,1}(k) & \dots & h_{1,M}(k) \\ h_{2,1}(k) & \dots & h_{2,M}(k) \\ \vdots & \ddots & \vdots \\ h_{N,1}(k) & \dots & h_{N,M}(k) \end{bmatrix} \cdot \begin{bmatrix} x_1(k) \\ x_2(k) \\ \vdots \\ x_M(k) \end{bmatrix} + \begin{bmatrix} n_1(k) \\ n_2(k) \\ \vdots \\ n_N(k) \end{bmatrix}. \quad (14)$$

Suppose a matrix is decomposed as $H(k) = Q(k) \cdot R(k)$. The QR decomposition is a coordinate rotation that left multiplies the vector $Y(k)$ in Eq. (13) by $Q(k)^H$ to produce a sufficient statistic

$$Z(k) = \begin{bmatrix} z_1(k) \\ z_2(k) \\ \vdots \\ z_M(k) \end{bmatrix} = Q(k)^H \cdot Y(k) = R(k) \cdot X(k) + \hat{N}(k), \quad (15)$$

where $\hat{N}(k) = Q(k)^H \cdot N(k)$. Since $R(k)$ is an upper triangular matrix, $x_M(k)$ can be easily detected as $\Theta\left(\frac{z_M(k)}{r_{M,M}(k)}\right)$ where $\Theta(\frac{\eta}{r}) = \arg\min\left(|\eta - r \cdot s|\right)_{s \in \sum_{c=1}^{C} x_c}$. If we change the order of $X(k)$, the column order of $H(k)$ is also changed. For example, if we exchange the positions of $x_1(k)$ and $x_M(k)$, we can rewrite Eq. (14) as

$$\begin{bmatrix} y_1(k) \\ y_2(k) \\ \vdots \\ y_N(k) \end{bmatrix} = \begin{bmatrix} h_{1,M}(k) & \dots & h_{1,1}(k) \\ h_{2,M}(k) & \dots & h_{2,1}(k) \\ \vdots & \ddots & \vdots \\ h_{N,M}(k) & \dots & h_{N,1}(k) \end{bmatrix} \cdot \begin{bmatrix} x_M(k) \\ x_2(k) \\ \vdots \\ x_1(k) \end{bmatrix} + \tilde{N}(k) = H_1(k)X_1(k) + \tilde{N}(k), \quad (16)$$

where $H_1(k)$ is the channel matrix that exchanged the first and Mth columns, and $X_1(k)$ is the transmitted signal matrix that exchanged the first and Mth rows, respectively. The QR decomposition of $H_1(k)$ is given by

$$H_1(k) = Q_1(k) \cdot R_1(k), \quad (17)$$

where $R_1(k)$ is given by

$$R_1(k) = \begin{bmatrix} r_{1,1,1}(k) & r_{1,2,1}(k) & \dots & r_{1,M,1}(k) \\ 0 & r_{2,2,1}(k) & \dots & r_{2,M,1}(k) \\ \vdots & \vdots & \ddots & \vdots \\ 0 & 0 & \dots & r_{M,M,1}(k) \end{bmatrix}. \quad (18)$$

From Eqs. (16) and (17), we can obtain the different matrix compared with Eq. (15) as follows,

$$Z_1(k) = Q_1(k)^H \cdot Y(k) = R_1(k) \cdot X_1(k) + \check{N}(k). \quad (19)$$

From Eqs. (16), (17), and (18), we can also easily calculate $\tilde{x}_1(k)$ as

$$\tilde{x}_1(k) = \Theta\left(\frac{Q_1(k)_M^H \cdot Y(k)}{r_{M,M,1}(k)}\right). \quad (20)$$

where $Q(k)_M^H$ is the Mth row of $Q(k)^H$. Moreover, if we exchange the positions of $x_2(k)$ and $x_M(k)$, we also obtain the channel matrix $H_2(k)$ and calculate $\tilde{x}_2(k)$. In the same manner, we can calculate $Q_3(k), \dots, Q_{M-1}(k)$ and $R_3(k), \dots, R_{M-1}(k)$ with permuted channel matrix. The main point of this method is to reorder $X(k)$ such that the coordinate to be detected is in the last row, the order of other signals is unrestricted. As a result, the detected signals are given by

$$\begin{aligned} \tilde{x}_2(k) &= \Theta\left(\frac{Q_2(k)_M^H \cdot Y(k)}{r_{M,M,2}(k)}\right), \\ \tilde{x}_3(k) &= \Theta\left(\frac{Q_3(k)_M^H \cdot Y(k)}{r_{M,M,3}(k)}\right), \\ &\vdots \\ \tilde{x}_{M-1}(k) &= \Theta\left(\frac{Q_{M-1}(k)_M^H \cdot Y(k)}{r_{M,M,M-1}(k)}\right). \end{aligned} \quad (21)$$

Observing Eqs. (20), and (21), we can find a common rule for detecting the transmitted signals as follows

$$\begin{bmatrix} Q_1(k)_M^H \\ Q_2(k)_M^H \\ \vdots \\ Q_{M-1}(k)_M^H \\ Q(k)_M^H \end{bmatrix} \cdot Y(k) = \text{diag} \begin{bmatrix} r_{M,M,1}(k) \\ r_{M,M,2}(k) \\ \vdots \\ r_{M,M,M-1}(k) \\ r_{M,M}(k) \end{bmatrix} \cdot X(k) + \check{N}(k), \quad (22)$$

where diag[ϵ] puts ϵ on the main diagonal. Therefore, we can rewrite Eq. (22) as

$$\begin{aligned} Y(k) &= [Q_1(k)_M, Q_2(k)_M, \dots, Q_{M-1}(k)_M, Q(k)_M] \cdot \text{diag} \begin{bmatrix} r_{M,M,1}(k) \\ r_{M,M,2}(k) \\ \vdots \\ r_{M,M,M-1}(k) \\ r_{M,M}(k) \end{bmatrix} \cdot X(k) + \tilde{N}(k) \\ &= \hat{Q}(k) \cdot \hat{R}(k) \cdot X(k) + \tilde{N}(k), \end{aligned} \quad (23)$$

where $Q(k)_M$ is the Mth column of the $Q(k)$, since $Q_1(k), \cdots, Q_{M-1}(k), Q(k)$ are unitary matrices. From Eq. (23), we obtain $\hat{Q}(k)$ and $\hat{R}(k)$ with M times QR decompositions where $\hat{Q}(k)$ is a combination of Mth column of each QR decomposition with permuted channel matrix. However, $\hat{Q}^H(k)$ is required only once like QRD-M. Even though $\hat{Q}(k)$ is not orthogonal matrix, the convolutions of each row of $\hat{Q}(k)^H$ and $Y(k)$ correspond to the transmitted signals as

$$\hat{Z}(k) = \hat{Q}(k)^H \cdot Y(k) = \hat{R}(k) \cdot X(k) + \bar{N}(k). \quad (24)$$

Since the norm of each column of $Q\hat{(k)}$ is unity and $\hat{R}(k)$ is a diagonal matrix, $\hat{Z}(k) = \hat{Q}(k)^H \cdot Y(k)$ shows no noise enhancement in (24). The initially detected signal is given by

$$\hat{X}(k) = \arg\min \sum_{m=1}^{M} \left| \hat{z}_m(k) - \hat{r}_m(k) \cdot \overline{x}_m(k) \right|^2, \quad (25)$$

where $\hat{z}_m(k)$ is the m-th column of $\hat{Z}(k)$ in (24). From Eq. (12), the initially estimated CSI includes estimation errors due to interpolation of the discretely assigned pilot signals. To achieve an improved system performance, we use an iterative channel identification. From Eq. (25), we can make the replica signals using detected symbols, and then calculate the estimation error for the ψth iteration as

$$\varepsilon_{m,n,\psi}(k) = \sum_{i=N_p}^{N_p+N_{int}-1} \frac{\{y_n(k,i)/h_{m,n,\psi-1}(k) \cdot \hat{x}_{m,\psi-1}(k,i)\}}{N_{int}} \quad (26)$$

where N_{int} is the size of interleaving. By using (26), we can calculate the improved CSI as

$$h_{m,n,\psi}(k) = \varepsilon_{m,n,\psi}(k) \cdot h_{m,n,\psi-1}(k). \quad (27)$$

Observing Eq. (27), it is clear that the estimated CSI is more accurate than that of the initially estimated CSI as Eq. (12). Efficient channel coding is essential to reducing the required E_b/N_o for wireless access. It is well known that soft-decision decoding exhibits a large coding gain. However, there is a problem in that the log likelihood ratio (LLR) of the *a posteriori* probability (APP) for soft-decision decoding cannot be obtained when no surviving symbol replicas remain that contain either bit "1" or "-1." Therefore, in this paper, we investigates the likelihood function of APP in the proposed system for the subsequently employed soft-decision decoding [11]. The desired bit streams are calculated by using the symbol replica candidates and their Euclidian distances and using soft-decision decoding. The Euclidian distances of the kth subcarrier, the mth transmitted antenna, and the ψth iteration, $\hat{\Xi}_{m,\psi}(k)$, can be calculated as

$$\begin{aligned} \hat{\Xi}_{m,\psi}(k) &= \sum_{c=1}^{C} \hat{e}_{m,c,\psi}(k) \\ &= \sum_{c=1}^{C} \left| \hat{z}_m(k) - \hat{r}_{m,\psi}(k) \cdot x_{m,c}(k) \right|^2, \end{aligned} \quad (28)$$

where C is the number of symbol replica candidates, and $\hat{r}_{m,\psi}(k)$ is the modified term for the ψ iteration of $\hat{r}_m(k)$ due to Eq. (27). The log likelihood ratio (LLR) of the *a posteriori* probability (APP) for the b-th bit, kth subcarrier, the mth transmitted antenna, and the ψth iteration, $\Lambda_{m,b,\psi}(k)$, is calculated for the subsequently employed soft-decision decoding from (28) as

$$\Lambda_{m,b,\psi}(k) = \begin{cases} \sqrt{\lfloor \hat{\Xi}_{m,\psi}(k) \rfloor} - \sqrt{\lceil \hat{\Xi}_{m,\psi}(k) \rceil} & \lfloor \hat{x}_{m,\psi}(k) \rfloor_b \geq 0 \\ \sqrt{\lceil \hat{\Xi}_{m,\psi}(k) \rceil} - \sqrt{\lfloor \hat{\Xi}_{m,\psi}(k) \rfloor} & \lfloor \hat{x}_{m,\psi}(k) \rfloor_b < 0, \end{cases} \quad (29)$$

where $\lfloor \hat{x}_{m,\psi}(k) \rfloor_b$ is the hard decision b-th bit for k-th subcarrier from the mth transmitter antenna and the ψth iteration, $\lfloor \hat{\Xi}_{m,\psi}(k) \rfloor$ and $\lceil \hat{\Xi}_{m,\psi}(k) \rceil$ are the minimum and maximum Euclidian distances among the surviving symbols for the kth subcarrier from the mth transmitted antenna and the ψth iteration, respectively.

3. Computer Simulated Results

Figure 1 shows a simulation model of the proposed MIMO/OFDM system with $N_c = 64$ subcarriers. On the transmitter side, the data stream is firstly encoded. Here, convolutional codes (rate $\mathcal{R} = 1/2$, constraint length $\xi = 7$) with bit interleaving are used. The interleaving size is 5 symbols duration. These have been found to be efficient for transmission of an OFDM signal over a frequency selective fading channel [18], [19]. The coded bits are QPSK modulated and then serial-to-parallel (S/P) transformed. Pilot signals are generated and assigned as shown in Fig. 2. The OFDM time signals are generated by an IFFT and transmitted from each transmit antenna element over the frequency selective and time variant radio channel after cyclic extensions have been inserted. The transmitted signals are subject to broadband channel propagation. In this model, $L = 15$ path Rayleigh fadings have exponential shapes with path separation $T_{path} = 125ns$. This situation causes a severe frequency selective fading. The normalized Doppler frequency is assumed to be $f_dT = 2 \cdot 10^{-3}$ and 10^{-4} where f_d is the Doppler frequency. In the receiver, the guard interval is erased from the received signals and the received signals are S/P converted. N_c parallel sequences are passed to an FFT operator, which converts the signal back to the frequency domain. The CSI is initially calculated by Eq. (12). The frequency domain signals are detected by a parallel detection algorithm using MQRD-PCM [12]. After a signal detection, the improved CSI is calculated by Eq. (27). In this simulation, the packets consist of 64 subcarriers and 22 OFDM

Table 1 Simulation parameters.

Modulation	QPSK
Effective data rate	8 Msymbol/s
Number of carriers	$N_c = 64$
Guard interval	16 sample times
Frame size	22 symbols ($N_p = 2$, $N_d = 20$)
FEC	Convolutional code ($\mathcal{R} = 1/2$, $\xi = 7$)
Fading	15 path Rayleigh fading
Normalized Doppler frequency	$f_dT = 2 \cdot 10^{-3}$, 10^{-4}
Antennas	M = 4, N = 4

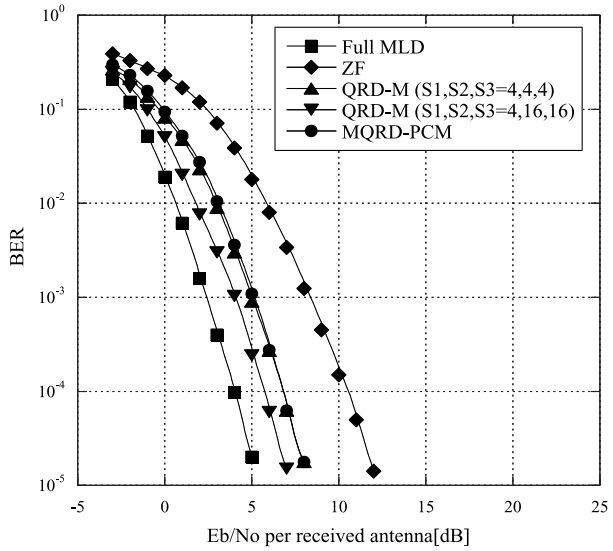

Fig. 3 BER of the full MLD-based MIMO, ZF-based MIMO, QRD-M based MIMO, and the MQRD-PCM based MIMO system with M = 4, N = 4 and $f_dT = 10^{-4}$.

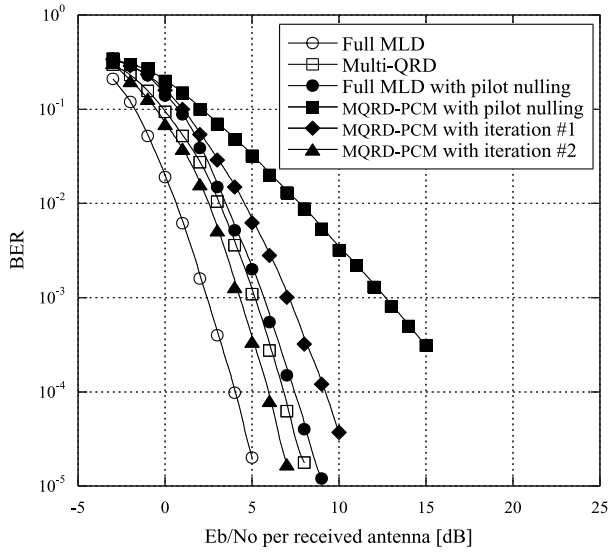

Fig. 4 BER of the full MLD-based MIMO, the MQRD-PCM-based MIMO with discrete pilot signal assignment and an iterative channel identification for M = 4, N = 4 at $f_dT = 10^{-4}$.

symbols for $M = 4$, $N = 4$. Table 1 shows the simulation parameters.

Figure 3 shows the BER of the full MLD-based MIMO, ZF-based MIMO, QRD-M based MIMO, and the MQRD-PCM based MIMO system with M = 4, N = 4 and $f_dT = 10^{-4}$. In the ZF-based MIMO, the detected signals include enhanced noise components. However, in MQRD-PCM based MIMO system, the calculated $\hat{Q}(k)$ is a unitary matrix, so there are no enhanced noised terms. For this reason, MQRD-PCM based MIMO system achieved a better BER than the ZF-based MIMO. The performance of the QRD-M depends on the number of surviving symbol replica candidates. With a small number of surviving candidates in the QRD-M, it is difficult to include the desired signal in the surviving symbol replica candidates every time. Meanwhile, with a large number of surviving candidates in the QRD-M, it is easy to include the desired signal in the surviving symbol replica candidates. Thus, the MQRD-PCM based MIMO system achieves the approximately same BER and 0.8 dB penalty at BER of 10^{-4} compared with QRD-M $(S_1, S_2, S_3 = 4, 4, 4)$ and QRD-M $(S_1, S_2, S_3 = 4, 16, 16)$ where S_m is the surviving symbol replica candidates for the mth stage of M-algorithm corresponding to transmitted signal from the mth transmit antenna. The full MLD produces the best BER performance. This is because the proposed scheme depends on the channel estimation property, on the other hand, the full MLD calculates all possible transmitted signals.

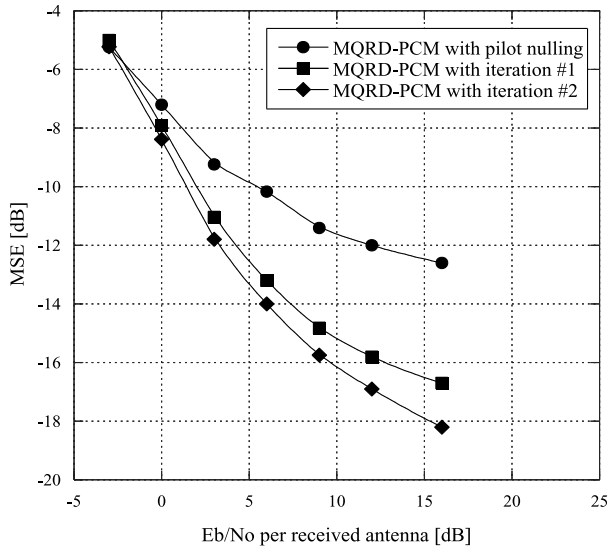

Fig. 5 MSE of the MQRD-PCM-based MIMO with discrete pilot signal assignment and an iterative channel identification for M = 4, N = 4 at $f_dT = 10^{-4}$.

Figure 4 shows the BER of the full MLD-based MIMO, the MQRD-PCM-based MIMO with discrete pilot signal assignment and an iterative channel identification for M = 4, N = 4 at $f_dT = 10^{-4}$. With discrete pilot signal assignment, the BER performance of the full MLD-based MIMO and MQRD-PCM-based MIMO shows the performance degradation compared with the the full MLD-based MIMO without discrete pilot signal assignment. Particularly, the BER of MQRD-PCM-based MIMO is significantly degraded compared with the full MLD-based MIMO. This is because MQRD-PCM-based MIMO depends on the accuracy of $\hat{Q}(k)$. However, $\hat{Q}(k)$ includes the imperfect CSI due to the pilot frequency interpolation. MQRD-PCM-based MIMO with iteration #2 can achieve 1.2 dB, 9 dB and 3.2 dB gains compared with full MLD-based MIMO and MQRD-PCM-based MIMO with discrete pilot signal assignment, and MQRD-PCM-based MIMO with iteration #1 for satisfying the BER of 10^{-3}. This is because the estimated CSI with iteration is more accurate than that of the initially esti-

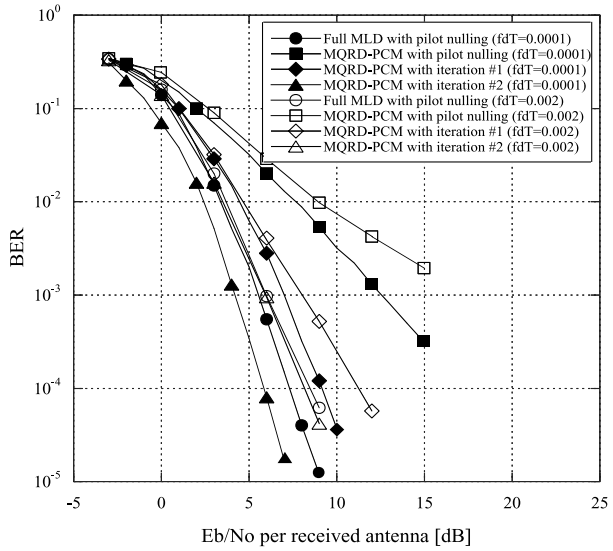

Fig. 6 BER of the full MLD-based MIMO, the MQRD-PCM-based MIMO with discrete pilot signal assignment and an iterative channel identification for M = 4, N = 4 at $f_dT = 2 \cdot 10^{-3}$ and 10^{-4}.

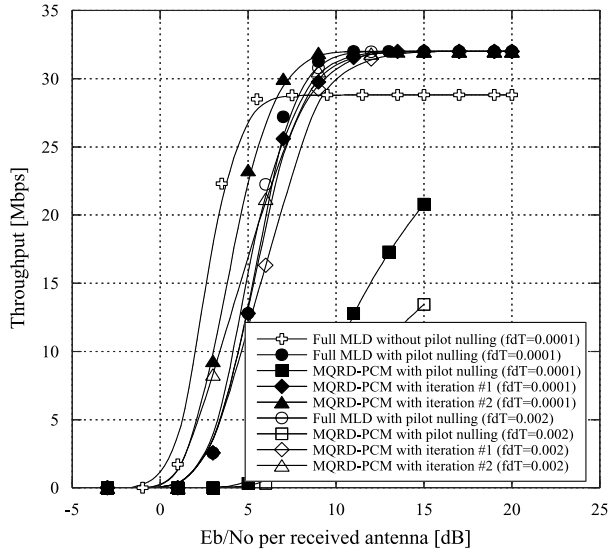

Fig. 7 Throughput of the full MLD-based MIMO and the MQRD-PCM-based MIMO for M = 4, N = 4 at $f_dT = 2 \cdot 10^{-3}$ and 10^{-4}.

mated CSI as shown in Fig. 5.

Figure 6 shows the BER of the full MLD-based MIMO, the MQRD-PCM-based MIMO with discrete pilot signal assignment and an iterative channel identification for M = 4, N = 4 at $f_dT = 2 \cdot 10^{-3}$ and 10^{-4}. By increasing the Doppler frequency, the BER performance of the MQRD-PCM-based MIMO is rapidly degraded compared with the full MLD-based MIMO. This is because $\hat{Q}(k)$ includes the imperfect CSI due to the pilot frequency interpolation and channel variance. In this case, iterative processing is also poorly operated. Therefore, the BER of full MLD-based MIMO and MQRD-PCM-based MIMO with iteration #2 show the approximately same BER.

Table 2 Required multiplication per packet.

Detection scheme	Required multiplication
Full MLD	Gen. of replica candidates $(4M^2CN_c)$ Squared Euclidian dist. $(2MC^MN_cN_d)$
QRD-M	QR-decom. of H $(4M^3N_c)$ Q^H $(4M^2N_cN_d)$ Squared Euclidian dist. $(2(1+\sum_{m=1}^{M-1}S_m)CN_cN_d)$
MQRD-PCM	QR-decom. of H $(4M^4N_c)$ Q^H $(4M^2N_cN_d)$ Squared Euclidian dist. $(2MCN_cN_d)$
MQRD-PCM with pilot nulling and iter. $(\psi > 0)$	QR-decom. of H $(4M^4N_c(\psi+1))$ Q^H $(4M^2N_cN_d(\psi+1))$ Gen. of replica candidates $(4M^2CN_c\psi)$ Squared Euclidian dist. $(2MCN_c(N_d+N_{int}\psi))$

Figure 7 shows the throughput of the full MLD-based MIMO and the MQRD-PCM-based MIMO for M = 4, N = 4 at $f_dT = 2 \cdot 10^{-3}$ and 10^{-4}. Since the full MLD-based MIMO without discrete pilot signal assignment uses many pilot symbols to distinguish all the CSI, the total transmission rate is degraded. On the other hand, the full MLD-based MIMO and MQRD-PCM-based MIMO with discrete pilot signal assignment use the reduced pilot symbols. As a result, in high E_b/N_o, the MQRD-PCM-based MIMO with discrete pilot signal assignment and an iterative channel identification achieve a significant improved throughput. By increasing the Doppler frequency, the performance behavior of MQRD-PCM-based MIMO with discrete pilot signal assignment and an iterative channel identification remains unchanged as the case with low Doppler frequency.

Table 2 shows the required multiplication per packet. C is the constellation size (QPSK). From Table 2, the total required multiplications per packet of the full MLD, QRD-M $(S_1, S_2, S_3 = 4, 16, 16)$, QRD-M $(S_1, S_2, S_3 = 4, 4, 4)$, the MQRD-PCM, and the MQRD-PCM-based MIMO with iteration #1 and #2 are 2637824, 477184, 231426, 188416, 362496, and 536576, respectively. Therefore, the required multiplication per packet of the MQRD-PCM is reduced about 1.3, 2.5 and 14 times when compared with QRD-M $(S_1, S_2, S_3 = 4, 4, 4)$, QRD-M $(S_1, S_2, S_3 = 4, 16, 16)$ and the full MLD, respectively. Moreover, the MQRD-PCM-based MIMO with iteration #2 can achieve the throughput improvement with reducing the complexity compared with the full MLD.

4. Conclusion

In this paper, we have evaluated the performance of parallel detection algorithm using MQRD-PCM-based MIMO. For increasing the total throughput performance, we consider the discrete pilot signal assignment and an iterative channel identification for MQRD-PCM-based MIMO. From the simulation results, the MQRD-PCM-based MIMO with iteration #2 can achieve 1.2 dB, 9 dB and 3.2 dB gains compared with full MLD-based MIMO and MQRD-PCM-based MIMO with discrete pilot signal assignment, and MQRD-PCM-based MIMO with iteration #1 for satisfying the BER

of 10^{-3}.

References

[1] A.V. Zelst, R.V. Nee, and G. Awater, "Space division multiplexing (SDM) for OFDM systems," Proc. Vehicular Technology Conference (VTC2000), vol.1, pp.15–18, 2000.
[2] A. Nallanathan and C. Yun, "Eigenbeam- space division multiplexing for OFDM systems with optimum resource allocation," Proc. Globecom2004, vol.4, pp.2366–2370, 2004.
[3] Y. Teng, K. Mori, and H, Kobayashi, "Complexity reduced maximum likelihood detection for SDM-OFDM system," Proc. Wireless Communications and Networking (WCNC 2005), vol.1, pp.256–261, 2005.
[4] P. Vandenameele, L.V. Perre, M.G.E. Engels, B. Gyselinck, and H.D. Man, "A combined OFDM/SDMA approach," IEEE J. Sel. Areas Commun., vol.18, no.11, pp.2312–2321, 2000.
[5] Y. Nouda, T. Koike, and S. Yoshida, "Iterative MLD equalizer preceded by MIMO-FDE for wideband spatial multiplexing systems," Proc. Vehicular Technology Conference (VTC2004), vol.1, pp.533–537, 2005.
[6] K.B. Letaif, E. Choi, J. Ahn, and R. Chen, "Joint maximum likelihood detection and interference cancellation for MIMO/OFDM systems," Proc. Vehicular Technology Conference (VTC2003), vol.1, pp.612–616, 2003.
[7] K. Kim, J. Yue, R. Iltis, and J. Gibson, "A QRD-M/Kalman filter-based detection and channel estimation algorithm for MIMO-OFDM systems," IEEE Trans. Wireless Communications, vol.4, no.2, pp.710–721, March 2005.
[8] Y. Dai, S. Sun, and Z. Lei, "A comparative study of QRD-M detection and sphere decoding for MIMO-OFDM systems," Proc. Personal, Indoor and Mobile Radio Communications (PIMRC2005), vol.1, pp.186–190, Sept. 2005.
[9] Y. Guo and D. McCain, "Reduced QRD-M detector in MIMO-OFDM systems with partial and embedded sorting," Proc. Globecom2005, vol.1, 2005.
[10] K. Higuchi, H. Kawai, N. Maeda, H. Taoka, and M. Sawahashi, "Experiments on real-time 1-Gb/s packet transmission using MLD-based signal detection in MIMO-OFDM broadband radio access," IEEE J. Sel. Areas Commun., vol.24, no.6, pp.1141–1153, 2006.
[11] H. Kawai, K. Higuchi, N. Maeda, M. Sawahashi, T. Ito, Y. Kakura, A. Ushirokawa, and H. Seki, "Likelihood function for QRM-MLD suitable for soft-decision turbo decoding and its performance for OFCDM MIMO multiplexing in multipath fading channel," IEICE Trans. Commun., vol.E88-B, no.1, pp.47–57, Jan. 2005.
[12] C. Ahn, "Parallel detection algorithm using multiple QR-decompositions with permuted channel matrix for MLD-SDM/OFDM," IEEE Trans. Veh. Technol., vol.57, no.4, July 2008.
[13] S. Serbetli and A.A.V. Yener, "MMSE transmitter design for correlated MIMO systems with imperfect channel estimates: Power allocation trade-offs," IEEE Trans. Wireless Communications, vol.5, no.8, pp.2295–2304, 2006.
[14] C. Pirak, Z. Wang, K. Liu, and S. Jitapunkul, "Adaptive channel estimation using pilot-embedded data-bearing approach for MIMO-OFDM systems," IEEE Trans. Signal Process., vol.54, no.12, pp.4706–4716, Dec. 2006.
[15] Y. You, M. Kim, S. Hong, I. Hwang, and H. Song, "Performance investigation of STBC-OFDM with code-division multiplexing in time-varying channels," IEEE Trans. Broadcast., vol.50, no.4, pp.408–413, Dec. 2004.
[16] L. Huang, K. Zheng, and W. Wang, "Channel estimation based on delay-subspace filter for uplink of CDM-OFDMA system," IEEE International Symposium on Microwave, Antenna, Propagation and EMC Technologies for Wireless Communications (MAPE2005), vol.2, pp.1415–1418, 2005.
[17] T.S. Rappaport, Wireless Communication: Pronciple and Practice, Prentice-Hall, 1996.
[18] J. Cho, C. Yoon, N. Cho, H. Jun, and D. Hong, "Optimal weighting for ML decoding of convolution code in COFDM systems," Proc. VTC 2001 Spring, vol.2, pp.796–799, 2001.
[19] L. Lang, L. Cimini, and J.C. Chuang, "Comparison of convolutional and turbo codes for OFDM with antenna diversity in high-bit-rate wireless applications," IEEE Commun. Lett., vol.4, no.9, pp.277–279, Sept. 2000

Chang-Jun Ahn received the Ph.D. degree in the Department of Information and Computer Science in 2003 from Keio University, Japan. From 2001 to 2003, he was a research associate in the Department of Information and Computer Science, Keio University. From 2003 to 2006, he was with the Communication Research Laboratory, Independent Administrative Institution (now the National Institute of Information and Communications Technology). In 2006, he was on assignment at ATR Wave Engineering Laboratories. Currently, he is working at the Faculty of Information Sciences, Hiroshima City University. His current research interests include OFDM, digital communication, channel coding, and signal processing for telecommunications. He once served as an associate editor for Special Section on Multi-dimensional Mobile Information Network for the IEICE Trans. on Fundamentals. From 2005 to 2006, he was an expert committee member for emergence communication committee, Shikoku Bureau of Telecommunications, Ministry of Internal Affairs and Communications (MIC), Japan. Dr. Ahn received the ICF research grant award for Young Engineer in 2002 and the Funai Information Science Award for Young Scientist in 2003. He is a member of IET (formerly IEE), IEEE and the Korean Institute of Communication Science (KICS).